



Journal of the European Ceramic Society

journal homepage: www.elsevier.com/locate/jeurceramsoc



Crystal structure, mixture behavior, and microwave dielectric properties of novel temperature stable $(1-x)\text{MgMoO}_4 - x\text{TiO}_2$ composite ceramics

Haoran Zheng, Shihui Yu*, Lingxia Li*, Xaosong Lyu, Zheng Sun, Siliang Chen

School of Electronic and Information Engineering and Key Laboratory for Advanced Ceramics and Machining Technology of Ministry of Education, Tianjin University, Tianjin 300072, China

ARTICLE INFO

Article history:

Received 17 February 2017

Received in revised form 10 June 2017

Accepted 14 June 2017

Available online xxx

Keywords:

Composite

Microstructure

Microwave dielectric properties

Temperature stability

ABSTRACT

Novel temperature stable $\text{MgMoO}_4\text{-TiO}_2$ microwave dielectric ceramics were prepared by a solid state reaction process at low temperature (950°C). As TiO_2 content increases, the relative permittivity increases while the $Q \times f$ value decreases, and the variation mechanisms are proposed, respectively. The temperature coefficient of resonant frequency (τ_f) shifts to the positive direction as TiO_2 is added. The mixture mechanisms of τ_f value for two-phase composite materials are supposed. A near-zero τ_f value ($3.2 \text{ ppm}/^\circ\text{C}$) is obtained when $x=0.3$, with $\epsilon_r=9.13 \pm 0.03$ and $Q \times f=11,990 \text{ GHz}$. The $0.7\text{MgMoO}_4\text{-}0.3\text{TiO}_2$ composites are considered to be appropriate as a low temperature co-fired ceramic material for microwave wireless communication applications.

© 2017 Elsevier Ltd. All rights reserved.

1. Introduction

With the rapid development of high frequency communication industry, microwave dielectric ceramics have attracted much attention for a wide range of microwave component applications, including filters, resonators, antennas and waveguides [1–5]. In order to meet the needs of miniaturization and integration of microwave devices, the low temperature co-fired ceramic (LTCC) technology is considered as a promising method from the manufacturing point of view [6–8]. In general, microwave dielectric ceramics with low sintering temperature ($<960^\circ\text{C}$), high quality factor ($Q \times f$) value, and near-zero temperature coefficient of resonant frequency (τ_f) are required [9–11].

In recent years, AMoO_4 ($\text{A}=\text{Ba}, \text{Mg}, \text{Mn}$ and Zn) ceramics are found potential candidates for the microwave applications, due to the low sintering temperature ($\sim 900^\circ\text{C}$), low relative permittivity (7–9), and high quality factor ($>30,000 \text{ GHz}$) [12,13]. However, all of them exhibit large negative τ_f value ($-46 \text{ ppm}/^\circ\text{C}$ to $-87 \text{ ppm}/^\circ\text{C}$), which is not suitable for practical use. A near-zero temperature coefficient of resonant frequency can ensure the thermal stability of the microwave devices at different working temperatures [14]. In order to achieve near-zero τ_f , one of the effective meth-

ods is to add other compounds with opposite τ_f value. Rutile TiO_2 with large positive τ_f value ($+460 \text{ ppm}/^\circ\text{C}$) [15], has been successfully applied in some microwave dielectric ceramics with negative temperature coefficient of resonant frequency [16–20]. Furthermore, the mixture behavior of composite ceramics has significant influence on the adjustment of relative permittivity and τ_f value. Therefore, we have attempted to demonstrate a comprehensive study of $(1-x)\text{MgMoO}_4 - x\text{TiO}_2$ ceramic system.

In this work, the phase composition, microstructure and microwave dielectric properties of $(1-x)\text{MgMoO}_4 - x\text{TiO}_2$ ceramics were investigated as a function of TiO_2 content ($0 \leq x \leq 0.4$). The relationship between microstructure and microwave dielectric properties was investigated. The variation mechanisms of relative permittivity, $Q \times f$ value and τ_f value were proposed, respectively.

2. Experimental details

MgMoO_4 composition was prepared by a solid state reaction process with reagent-grade MgO and MoO_3 as raw materials. Powdered oxides were weighted in stoichiometry, and subsequently ball milled in ethanol for 6 h. After being dried under an infrared lamp, the mixture was calcined at 700°C in alumina crucible for 6 h. MgMoO_4 and TiO_2 powders were mixed by ball-milling for 12 h according to the following formula: $(1-x)\text{MgMoO}_4 - x\text{TiO}_2$ ($x=0.0, 0.1, 0.2, 0.3$ and 0.4). The final powders were pressed into cylinders of 15 mm in diameter and 7 mm in thickness with 7 wt% wax as

* Corresponding authors.

E-mail addresses: ysh728@126.com (S. Yu), lingxiali66@163.com (L. Li).

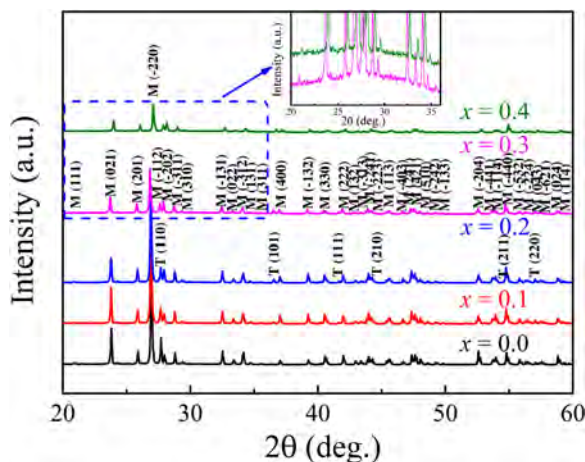


Fig. 1. X-ray diffraction patterns of $(1-x)\text{MgMoO}_4 - x\text{TiO}_2$ ceramics sintered at 950°C (M: MgMoO_4 phase; T: TiO_2 phase).

a binder. After burning off the binder at 550°C , the samples were sintered at 950°C in air for 5 h.

The crystalline structures of the samples were identified by an X-ray diffractometer (Rigaku Ultima IV, Japan) with $\text{Cu K}\alpha$ radiation over a 2θ angle from 20° to 60° . The microstructure of polished and etched surfaces was analyzed with field emission scanning electron microscopy (FE-SEM, ZEISS MERLIN Compact, Germany). The bulk density of samples was measured using the Archimedes' method. The microwave dielectric properties of the sintered samples were measured using a network analyzer (Agilent, 8720ES, Santa Clara, California). The relative permittivity and unloaded Q value were measured by the Hakk-Coleman method and shielded cavity method, respectively. The temperature coefficient of resonant frequency was determined in the temperature range of 25°C - 85°C using the equation:

$$\tau_f = \frac{f_2 - f_1}{f_1(85 - 25)} \times 10^6 \text{ (ppm/}^\circ\text{C}) \quad (1)$$

where f_1 and f_2 are the resonant frequency at 25°C and 85°C .

3. Results and discussion

Fig. 1 illustrates the XRD patterns of $(1-x)\text{MgMoO}_4 - x\text{TiO}_2$ ceramics sintered at 950°C . No phase other than MgMoO_4 (JCPDS #21-0961) is detected for $x=0$, implying that all the raw materials react completely to form a solid solution. MgMoO_4 performs monoclinic wolframite structure and belongs to the space group C2/m (no.12) and $Z=8$ [21]. The lattice parameters are $a=10.281\text{\AA}$, $b=9.291\text{\AA}$, and $c=7.030\text{\AA}$. Rutile TiO_2 (JCPDS #21-1276) coexisting with MgMoO_4 can be seen from $x=0.1$ to 0.4 , which indicates that they behave as a mixture. With the increase of x , the intensities of MgMoO_4 diffraction peaks initially increase but subsequently decrease, and become strongest when $x=0.1$. The phenomena suggest that appropriate TiO_2 can promote MgMoO_4 in the mass transfer and sintering process, however, excessive TiO_2 will lead to the deterioration of crystal quality for MgMoO_4 . In addition, a bump can be observed from the inset for $x=0.3$ and 0.4 , indicating the appearance of amorphous TiO_2 . The relative volume fraction of rutile phase can be defined as the ratio of the most-intense XRD peak height of TiO_2 to the sum of the most-intense peak heights of TiO_2 and MgMoO_4 [22]. The calculated proportions of TiO_2 phase are 0.055, 0.077, 0.129, and 0.165 for $x=0.1, 0.2, 0.3$, and 0.4 respectively.

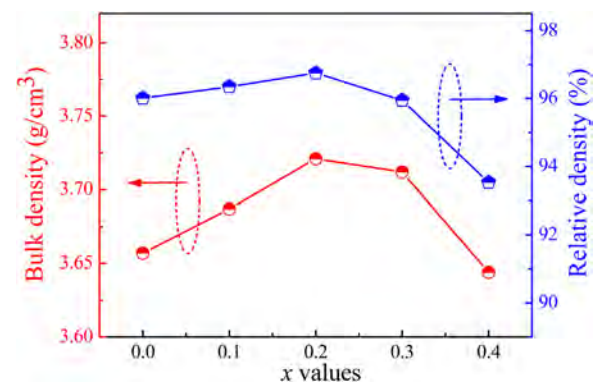


Fig. 2. Bulk density and relative density of $(1-x)\text{MgMoO}_4 - x\text{TiO}_2$ ceramics with various x values.

tively. The volume fraction of TiO_2 is related to the x value, which obeys the following equation [23]:

$$v_T = \frac{xM_T/\rho_T}{xM_T/\rho_T + (1-x)M_M/\rho_M} \quad (2)$$

where ρ_T and ρ_M are the density of TiO_2 and MgMoO_4 , respectively. M_T and M_M represent the relative molecular mass of TiO_2 and MgMoO_4 , respectively. The volume fractions of TiO_2 are 0.040, 0.086, 0.138, and 0.200 for $0.1 \leq x \leq 0.4$. When $x=0.1$, the obtained content of TiO_2 from XRD is larger than the designed value. This is attributed to the lower actual density of TiO_2 . Whereas, the calculated values of others are lower than the designed values, which may be due to the emergence of amorphous TiO_2 and pores in the ceramics.

Fig. 2 exhibits the bulk density and relative density of $(1-x)\text{MgMoO}_4 - x\text{TiO}_2$ ceramics sintered at 950°C . As TiO_2 content increases, the bulk density gradually increases from 3.657 g/cm^3 to 3.721 g/cm^3 for $0 \leq x \leq 0.2$, due to the higher theoretical density of TiO_2 (4.230 g/cm^3) than MgMoO_4 (3.809 g/cm^3). However, with a further increase of TiO_2 content ($x \geq 0.3$), the bulk density decreases. This may result from the rise in porosity due to the excess TiO_2 . To study the relative density of $(1-x)\text{MgMoO}_4 - x\text{TiO}_2$ ceramics, the theoretical density is obtained according to the formula [24]:

$$TD_{M-T} = \frac{W_M + W_T}{W_M/TD_M + W_T/TD_T} \quad (3)$$

where TD_{M-T} , TD_M , and TD_T are the theoretical density of $(1-x)\text{MgMoO}_4 - x\text{TiO}_2$, MgMoO_4 and TiO_2 , respectively. W_M and W_T represent the weight percentage of MgMoO_4 and TiO_2 in the mixture. Eq. (3) is valid since no interaction takes place between MgMoO_4 and TiO_2 , which is confirmed by the phase analysis. The calculated theoretical densities are 3.827 g/cm^3 , 3.846 g/cm^3 , 3.869 g/cm^3 and 3.896 g/cm^3 for $x=0.1, 0.2, 0.3$, and 0.4 , respectively. The relative density is obtained from

$$\rho_{\text{relative}} = \frac{\rho_{\text{bulk}}}{\rho_{\text{theoretical}}} \times 100\% \quad (4)$$

As shown in **Fig. 2**, the relative density steadily increases from 96.0% to 96.7% for $0 \leq x \leq 0.2$, but subsequently decreases to 93.5% for $x=0.4$. The variation trends of bulk density and relative density along with x are consistent with the XRD results.

The microstructures of $(1-x)\text{MgMoO}_4 - x\text{TiO}_2$ ceramics sintered at 950°C are further analyzed by SEM. As shown in **Fig. 3(a)**, pores are hardly found in pure MgMoO_4 sample. However, some indistinct grain boundaries can be observed, which may attribute to the partial melting of the samples sintered at 950°C . This would have a harmful effect on the grain growth process. When $x=0.1$, rod-shaped TiO_2 grains with a width size of $0.5\text{ }\mu\text{m}$ appear for the

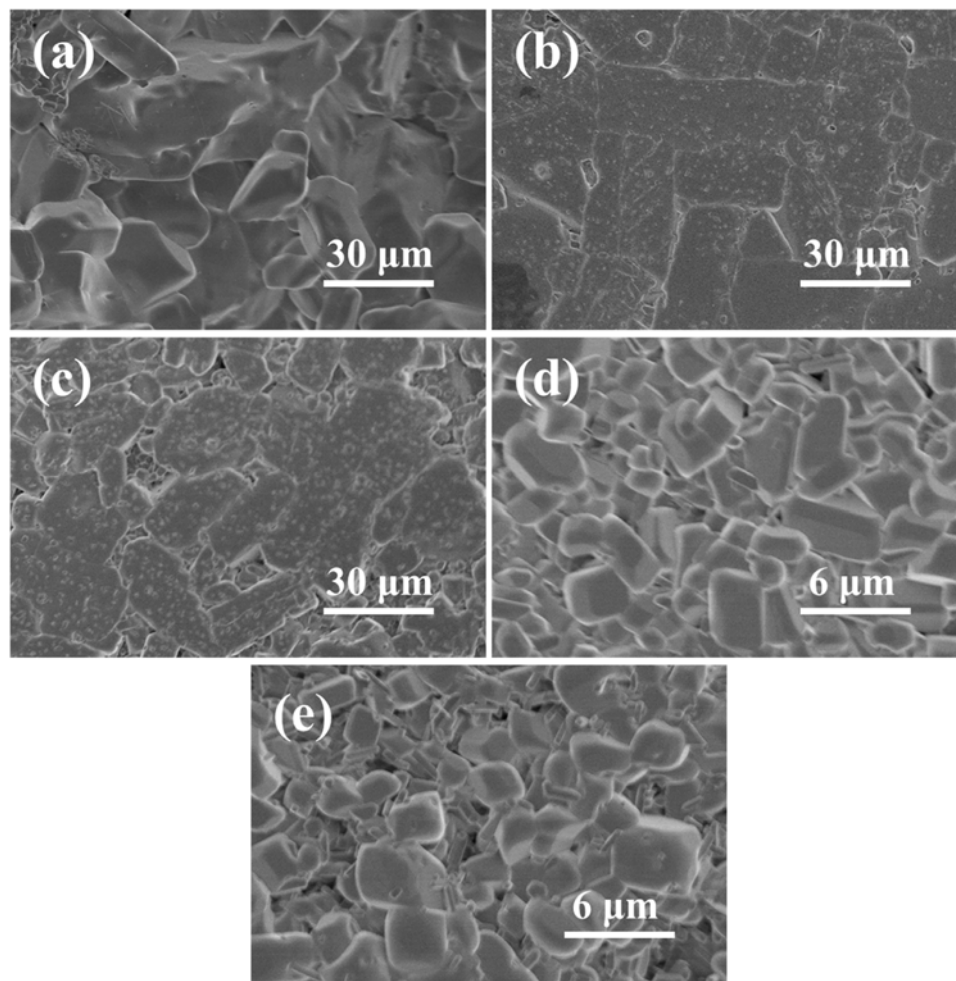


Fig. 3. SEM images of $(1-x)\text{MgMoO}_4 - x\text{TiO}_2$ ceramics sintered at 950°C : (a) $x=0$, (b) $x=0.1$, (c) $x=0.2$, (d) $x=0.3$, and (e) $x=0.4$.

first time in Fig. 3(b), and increase along with x . The two types of grains (MgMoO_4 and TiO_2) are randomly distributed, which consists well with the discussions above. The average grain size of MgMoO_4 is estimated using linear intercept method as follows [25]:

$$D = \frac{3L}{2MN} \quad (5)$$

where D , L , M and N represent the grain size, the length of test line, the magnification and the number of intercepts which grain boundaries make with the line. The calculated results are $18.3\text{ }\mu\text{m}$ and $23.1\text{ }\mu\text{m}$ for $x=0$ and 0.1 , respectively, indicating that the introduction of TiO_2 can promote the grain growth of MgMoO_4 . However, with a further increase of x , the average grain size of MgMoO_4 decreases from $17.6\text{ }\mu\text{m}$ to $2.6\text{ }\mu\text{m}$ for $0.2 \leq x \leq 0.4$. It also can be seen from Fig. 3(d) and (e) that, abnormal grains and pores are formed in sintered samples, leading to a decrease of density. This demonstrates that excess TiO_2 have no benefits to the densification of $(1-x)\text{MgMoO}_4 - x\text{TiO}_2$ ceramics.

Such changes in the microstructure are related to the different physical and chemical properties that depend on different TiO_2 contents of the samples. Pure MgMoO_4 ceramics are well sintered at 900°C [12]. As the sintering temperature increases to 950°C , the samples are slightly over sintered and a small amount of liquid melt is formed in the grain boundaries. However, the liquid melt can effectively decrease the sintering temperature of TiO_2 by increasing grain boundary motion, diffusion and crystallization kinetics [26]. Therefore, the grain growth of TiO_2 is promoted. At the same time, due to the movement of liquid melt, the crystal quality of MgMoO_4

becomes better and the average grain size increases. Evidently, MgMoO_4 and TiO_2 can positively influence each other during their sintering process. With a further increase of TiO_2 content, the liquid melt is insufficient for the sintering of excess TiO_2 , which exists as amorphous state in $(1-x)\text{MgMoO}_4 - x\text{TiO}_2$ ceramics. This leads to the deterioration of crystallization for both the two phases and the decrease of density. The discussions correspond well with the variation of microstructure.

Considering the relatively high relative permittivity of TiO_2 ($\varepsilon_r = 105$), the relative permittivity of $(1-x)\text{MgMoO}_4 - x\text{TiO}_2$ samples is expected to increase along with the TiO_2 content. Fig. 4 depicts the relative permittivity of $(1-x)\text{MgMoO}_4 - x\text{TiO}_2$ ceramics sintered at 950°C as a function of x value. It can be observed that as x rises, the measured relative permittivity gradually increases from 6.73 ± 0.04 to 9.97 ± 0.06 for $0 \leq x \leq 0.4$.

In composite ceramics, the relative permittivity is determined by the permittivity, volume fraction, and complex form of the component material. Many researchers have studied the dielectric response of two-phase compounds and proposed different models and equations [27–29]. The Licktenecher equation is the most widely used empirical equation to predict the relative permittivity of two-phase ceramics by the following relation [30]:

$$\varepsilon^\alpha = (1 - \nu)\varepsilon_1^\alpha + \nu\varepsilon_2^\alpha \quad (6)$$

where ε_i is the relative permittivity of the i th material and ν represents the volume fraction of material 2. The parameter α varies from -1 to 1 , determined by the complex model. The serial model,

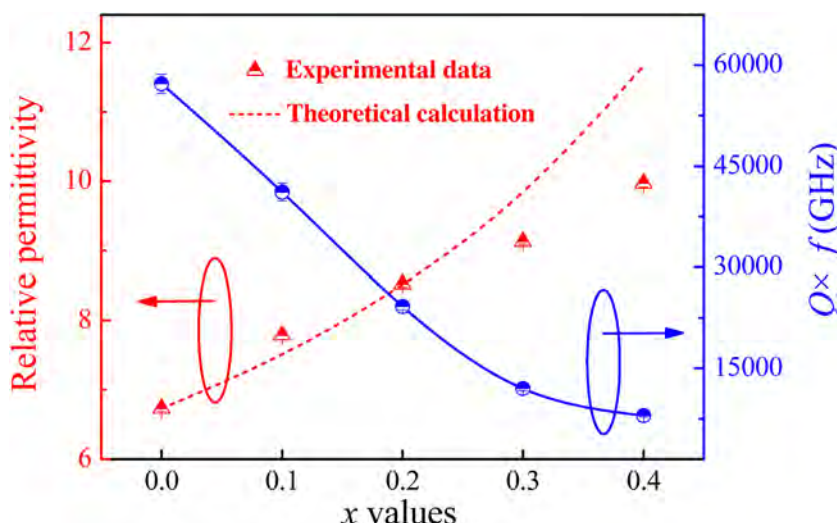


Fig. 4. Relative permittivity and $Q \times f$ value of $(1-x)\text{MgMoO}_4 - x\text{TiO}_2$ ceramics with various x values.

logarithmic rule model and parallel model correspond to $\alpha = -1, 0$ and 1 , respectively. Among the three complex models, the logarithmic rule model is used for randomly distributed composite systems, which better fits the measured data [31].

$$\log \varepsilon = (1 - \nu) \log \varepsilon_1 + \nu \log \varepsilon_2 \quad (7)$$

The simulation curve is presented in Fig. 4. The relative permittivity of MgMoO_4 and TiO_2 are $\varepsilon_1 = 6.73$ and $\varepsilon_2 = 105$, respectively. It can be seen that when $x \leq 0.2$, the calculated relative permittivity is in good agreement with the experimental value. The measured result for $x = 0.1$ is a little higher than the theoretical relative permittivity, which attributes to the larger actual proportion of TiO_2 . However, a deviation from the fitting curve can be observed for $x = 0.3$ and 0.4 . This is mainly due to the low relative permittivity of amorphous TiO_2 and pores, well consistent with the microstructure analysis results.

The measured $Q \times f$ value of $(1-x)\text{MgMoO}_4 - x\text{TiO}_2$ ceramics sintered at 950°C is shown in Fig. 4. It is observed that with increasing the TiO_2 content, the $Q \times f$ value decreases monotonously in the entire composition range. The maximum $Q \times f$ is $57,240$ GHz ($x = 0$) and minimum $Q \times f$ is 7980 GHz ($x = 0.4$). In general, the $Q \times f$ value is affected by two parts: intrinsic losses and extrinsic losses. The intrinsic losses are caused by absorptions of phonon oscillation and the extrinsic losses are influenced by many factors, such as impurity, defect concentration, grain size, grain boundaries, and pores, etc [32]. In the $(1-x)\text{MgMoO}_4 - x\text{TiO}_2$ composites, the extrinsic factors are dominated. Because of few impurities and defects, the variation trend of $Q \times f$ value is dependent on other factors. When TiO_2 is added to MgMoO_4 , the $Q \times f$ value for $x = 0.1$ decreases, owing to the formation of grain boundaries between the two phases. With a further increase of TiO_2 content, the average grain size of MgMoO_4 decreases, resulting in the increase of grain boundaries per unit volume. In addition, accompanied with the excess TiO_2 , pores are generated for $x \geq 0.3$. These are the sources of loss which will lead to the large dielectric loss, therefore, the $Q \times f$ value decreases along with x .

Fig. 5 shows the temperature coefficient of resonant frequency of $(1-x)\text{MgMoO}_4 - x\text{TiO}_2$ ceramics sintered at 950°C . The measured τ_f value shifts from -79.7 ppm/ $^\circ\text{C}$ to 24.6 ppm/ $^\circ\text{C}$ with the increase of x from 0 to 0.4 , and a near-zero τ_f value (3.2 ppm/ $^\circ\text{C}$) is obtained when $x = 0.3$.

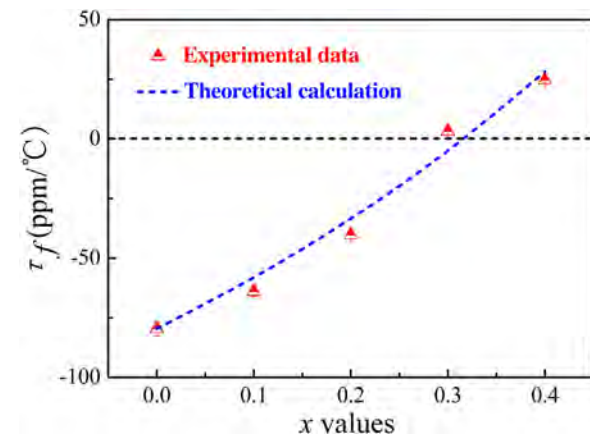


Fig. 5. Temperature coefficient of resonant frequency of $(1-x)\text{MgMoO}_4 - x\text{TiO}_2$ ceramics with various x values.

As well known, τ_f is affected by the additive, composition and second phase. It can be written as follows [33]:

$$\tau_f = -\left(\frac{\tau_\varepsilon}{2} + \alpha_L\right) \quad (8)$$

where τ_ε and α_L represent the temperature coefficient of relative permittivity and linear thermal expansion coefficient, respectively. In two-phase composite ceramics, the τ_ε can be further defined by a mathematical derivation based on Eq. (7) [34]:

$$\frac{d(\log \varepsilon)}{dT} = (1 - \nu) \frac{d(\log \varepsilon_1)}{dT} + \nu \frac{d(\log \varepsilon_2)}{dT} \quad (9)$$

$$\frac{1}{\varepsilon} \frac{d\varepsilon}{dT} = (1 - \nu) \frac{1}{\varepsilon_1} \frac{d\varepsilon_1}{dT} + \nu \frac{1}{\varepsilon_2} \frac{d\varepsilon_2}{dT} \quad (10)$$

$$\tau_\varepsilon = (1 - \nu) \tau_{\varepsilon_1} + \nu \tau_{\varepsilon_2} \quad (11)$$

where τ_{ε_i} is the τ_ε value of the i th material. Since the linear thermal expansion coefficient of microwave dielectric is about 10 ppm/ $^\circ\text{C}$, the α_L value is assumed to be a constant. From Eqs. (8) and (11), the τ_f can be then described as:

$$\tau_f = (1 - \nu) \tau_{f_1} + \nu \tau_{f_2} \quad (12)$$

where τ_{f_1} and τ_{f_2} are the τ_f values of material 1 and material 2. The simulation curve of calculated τ_f value is plotted in Fig. 5. The τ_f of MgMoO_4 and TiO_2 are $\tau_{f_1} = -79.7$ ppm/ $^\circ\text{C}$ and $\tau_{f_2} = +460$ ppm/ $^\circ\text{C}$, respectively. The measured τ_f values are similar to the calculated

Table 1Microwave dielectric properties of 0.7MgMoO₄–0.3TiO₂ composites and other molybdate ceramics.

	Relative permittivity	$Q \times f$ (GHz)	τ_f (ppm/°C)	References
0.7MgMoO ₄ – 0.3TiO ₂	~9.1	11,990	3.2	This work
0.7MgMoO ₄	~6.7	57,273	-79.7	This work
ZnMoO ₄	8.67	49,900	-87.49	[12]
BaMoO ₄	9.0	37,110	-90.1	[23]
MnMoO ₄	8.55	54,100	-73.91	[12]

ones, which indicates that MgMoO₄ and TiO₂ are randomly mixed in the (1 - x)MgMoO₄ – x TiO₂ ceramics. The microwave dielectric properties of 0.7MgMoO₄–0.3TiO₂ composites are listed in Table 1. Compared with other molybdate ceramics, 0.7MgMoO₄–0.3TiO₂ composites present a near-zero temperature coefficient of resonant frequency, which is beneficial for LTCC applications.

4. Conclusions

(1 - x)MgMoO₄ – x TiO₂ ceramics were prepared by a solid state reaction method. The microstructure and microwave dielectric properties of the samples sintered at 950 °C are investigated. The XRD and SEM analyses reveal that rutile TiO₂ can coexist with wolframite MgMoO₄. With the increase of x , the relative permittivity gradually increases from 6.73 ± 0.04 to 9.97 ± 0.06 and the $Q \times f$ value monotonously decreases from 57,240 GHz to 7980 GHz. The deviation between measured relative permittivity and calculated value has a close relationship with the variation of microstructure. The variation mechanisms of relative permittivity and $Q \times f$ value are proposed, respectively. The τ_f value shifts from -79.7 ppm/°C to 24.6 ppm/°C along with the TiO₂ content. The mixture mechanisms of τ_f value for two-phase composite materials are supposed. A near-zero τ_f value (3.2 ppm/°C) is obtained for $x = 0.3$, with $\epsilon_r = 9.13 \pm 0.03$ and $Q \times f = 11,990$ GHz. The 0.7MgMoO₄ – 0.3TiO₂ composites are considered to be appropriate as a low temperature co-fired ceramic material for microwave wireless communication applications.

Acknowledgments

This work was supported financially by the National Natural Science Foundation of China (No. 61671326) and Independent Innovation Fund of Tianjin University (No. 1705).

References

- [1] E.S. Kim, B.S. Chun, R. Freer, R.J. Cernik, Effects of packing fraction and bond valence on microwave dielectric properties of $A^{2+}B^{6+}O_4$ (A^{2+} : Ca Pb, Ba; B^{6+} : Mo, W) ceramics, J. Eur. Ceram. Soc. 30 (2010) 1731–1736.
- [2] Y.C. Lee, J.D. Chiu, Y.H. Chen, Effects of Nb₂O₅ doping on the microwave dielectric properties and microstructures of Bi₂Mo₂O₉ ceramics, J. Am. Ceram. Soc. 96 (2013) 1477–1482.
- [3] Y. Zhang, Y.C. Zhang, M.Q. Xiang, Crystal structure and microwave dielectric characteristics of Zr-substituted CoTiNb₂O₈ ceramics, J. Eur. Ceram. Soc. 36 (2016) 1945–1951.
- [4] Q.S. Cao, W.Z. Lu, X.C. Wang, J.H. Zhu, B. Ulla, W. Lei, Novel zinc manganese oxide-based microwave dielectric ceramics for LTCC applications, Ceram. Int. 41 (2015) 9152–9156.
- [5] J. Zhang, R.Z. Zuo, Effect of ordering on the microwave dielectric properties of spinel-structured $(Zn_{1-x}(Li_{2/3}Ti_{1/3})_x)_2TiO_4$ ceramics, J. Am. Ceram. Soc. 99 (2016) 3343–3349.
- [6] A. Surjith, R. Ratheesh, High q ceramics in the ACe₂(MoO₄)₄ (A = Ba, Sr and Ca) system for LTCC applications, J. Alloy Compd. 550 (2013) 169–172.
- [7] L.X. Pang, H. Liu, D. Zhou, G.B. Sun, W.G. Qin, W.G. Liu, Microwave dielectric ceramic with intrinsic low firing temperature: baLa₂(MoO₄)₄, Mater. Lett. 72 (2012) 128–130.
- [8] M. Guo, G. Dou, S.P. Gong, D.X. Zhou, Low-temperature sintered MgWO₄-CaTiO₃ ceramics with near-zero temperature coefficient of resonant frequency, J. Eur. Ceram. Soc. 32 (2012) 883–890.
- [9] S.H. Yoon, D.W. Kim, S.Y. Cho, K.S. Hong, Investigation of the relations between structure and microwave dielectric properties of divalent metal tungstate compounds, J. Eur. Ceram. Soc. 26 (2006) 2051–2054.
- [10] S.D. Rama Rao, S. Roopas Kiran, V.R.K. Murthy, Correlation between structural characteristics and microwave dielectric properties of scheelite $Ca_{1-x}Cd_xMoO_4$ solid solution, J. Am. Ceram. Soc. 95 (2012) 3532–3537.
- [11] H.F. Zhou, J.Z. Gong, N. Wang, X.L. Chen, A novel temperature stable microwave dielectric ceramic with low sintering temperature and high quality factor, Ceram. Int. 42 (2016) 8822–8825.
- [12] G.K. Choi, J.R. Kim, S.H. Yoon, K.S. Hong, Microwave dielectric properties of scheelite (A = Ca, Sr Ba) and wolframite (A = Mg, Zn, Mn) AMoO₄ compounds, J. Eur. Ceram. Soc. 27 (2007) 3063–3067.
- [13] E.S. Kim, C.J. Jeon, P.G. Clem, Effects of crystal structure on the microwave dielectric properties of ABO₄ (A = Ni, Mg Zn and B = Mo, W) ceramics, J. Am. Ceram. Soc. 95 (2012) 2934–2938.
- [14] R.C. Kell, A.C. Greenham, G.C.E. Olds, High-permittivity temperature-stable ceramic dielectrics with low microwave loss, J. Am. Ceram. Soc. 56 (1973) 352–354.
- [15] X.S. Lyu, L.X. Li, S. Zhang, H. Sun, B.W. Zhang, J.T. Li, M.K. Du, Crystal structure and microwave dielectric properties of novel (1-x)ZnZrNb₂O₈-xTiO₂ ceramics, Mater. Lett. 171 (2016) 129–132.
- [16] J.L. Ma, T. Yang, Z.F. Fu, P. Liu, Q.Q. Feng, L.P. Zhao, Low-fired Mg₂SiO₄-based dielectric ceramics with temperature stable for LTCC applications, J. Alloy. Compd. 695 (2017) 3198–3201.
- [17] W. Wang, W.F. Bai, B. Shen, J.W. Zhai, Microwave dielectric properties of low temperature sintered ZnWO₄-TiO₂ composite ceramics, Ceram. Int. 41 (2015) S435–S440.
- [18] J. Guo, D. Zhou, H. Wang, X. Yao, Microwave dielectric properties of (1-x)ZnMoO₄-xTiO₂ composite ceramics, J. Alloy. Compd. 509 (2011) 5863–5865.
- [19] D.W. Kim, K.H. Ko, D.K. Kwon, K.S. Hong, Origin of microwave dielectric loss in ZnNb₂O₆-TiO₂, J. Am. Ceram. Soc. 85 (2002) 1169–1172.
- [20] B.C. Guo, P. Liu, T. Yang, H.W. Zhang, Thermal stable microwave dielectric properties of CdWO₄ ceramics prepared by high energy ball milling method, J. Alloy. Compd. 650 (2015) 777–782.
- [21] V.V. Bakakin, R.F. Klevtsova, L.A. Gaponenko, Crystal-structure of magnesium molybdate MgMoO₄—an example of modified closest packing with 2 types of tetrahedra, Kristallografiya 27 (1982) 38–42.
- [22] W. Lei, W.Z. Lu, J.H. Zhu, X.H. Wang, Microwave dielectric properties of ZnAl₂O₄-TiO₂ spinel-based composites, Mater. Lett. 61 (2007) 4066–4069.
- [23] J. Guo, D. Zhou, H. Wang, Y.H. Chen, Y. Zeng, F. Xiang, Y. Wu, X. Yao, Microwave and infrared dielectric response of temperature stable (1-x)BaMoO₄-xTiO₂ composite ceramics, J. Am. Ceram. Soc. 95 (2012) 232–237.
- [24] C.L. Huang, M.H. Weng, C.T. Lion, C.C. Wu, Low temperature sintering and microwave dielectric properties of Ba₂Ti₉O₂₀ ceramics using glass additions, Mater. Res. Bull. 35 (2000) 2445–2456.
- [25] K.C.B. Naidu, W. Madhuri, Microwave processed NiMg ferrite: studies on structural and magnetic properties, J. Magn. Magn. Mater. 420 (2016) 109–116.
- [26] B. Houng, S.J.J. Wu, S.H. Lu, W.C. Chien, Microstructure and properties evaluation of TiO₂ ceramics with multi-oxides glass additions, Ceram. Int. 40 (2014) 3731–3736.
- [27] V.O. Sherman, A.K. Tagantsev, N. Setter, D. Iddles, T. Price, Ferroelectric-dielectric tunable composites, J. Appl. Phys. 99 (2006) 074104.
- [28] K. Wakino, T. Okada, N. Yoshida, K. Tomono, A new equation for predicting the dielectric constant of a mixture, J. Am. Ceram. Soc. 76 (1993) 2588–2594.
- [29] M. Lei, The impact of composite effect on dielectric constant and tunability in ferroelectric-dielectric system, J. Am. Ceram. Soc. 98 (2015) 3250–3258.
- [30] H. He, Y.B. Xu, A unified equation for predicting the dielectric constant of a two phase composite, Appl. Phys. Lett. 104 (2014) 062906.
- [31] D.W. Kim, B. Park, J.H. Chung, K.S. Hong, Mixture behavior and microwave dielectric properties in the low-fired TiO₂-CuO system, Jpn. J. Appl. Phys. 39 (2000) 2696–2700.
- [32] S.J. Penn, N.M. Alford, A. Templeton, X.R. Wang, M.S. Xu, M. Reece, K. Schrapel, Effect of porosity and grain size on the microwave dielectric properties of sintered alumina, J. Am. Ceram. Soc. 80 (1997) 1885–1888.
- [33] T.W. Zhang, R.Z. Zuo, C. Zhang, Preparation and microwave dielectric properties of Li₃(Mg_{0.92}Zn_{0.08})₂NbO₆-Ba₃(VO₄)₂ composite ceramics for LTCC applications, Mater. Res. Bull. 68 (2015) 109–114.
- [34] L.X. Pang, H. Wang, D. Zhou, X. Yao, A new temperature stable microwave dielectric with low-firing temperature in Bi₂MoO₆-TiO₂ system, J. Alloy. Compd. 493 (2010) 626–629.